Biogeochemistry (2023) 166:247–268
https://doi.org/10.1007/s10533-023-01069-0

Nitrogen fixation facilitates stream microbial mat biomass across the McMurdo Dry Valleys, Antarctica

Tyler J. Kohler · Joel G. Singley · Adam N. Wlostowski · Diane M. McKnight

Received: 1 February 2023 / Accepted: 9 July 2023 / Published online: 19 July 2023

Abstract Nitrogen (N) fixation is a fundamental mechanism by which N enters streams. Yet, because of modern N saturation, it is difficult to study the importance of N-fixation to stream nutrient budgets. Here, we utilized relatively simple and pristine McMurdo Dry Valley streams to investigate the role of N-fixing *Nostoc* abundance, streamwater dissolved inorganic N (DIN) concentration, and distance from the source glacier in regulating the elemental and isotopic composition of three microbial mat types (black, orange, and green) at the landscape scale. We found *Nostoc*-based black mats were the most enriched in $\delta^{15}N$, and $\delta^{15}N$ signatures of mats increased where *Nostoc* was abundant, but did not surpass the atmospheric standard ($\delta^{15}N \approx 0‰$). Furthermore, green and orange mat $\delta^{15}N$ signatures became more depleted with increasing DIN, indicating that mats utilize glacial meltwater-sourced N when available. The distance from the source glacier explained limited variability in mat $\delta^{15}N$ across sites, indicating the influence of individual stream characteristics on N spiraling. To further explore longitudinal N spiraling processes generating observed $\delta^{15}N$ patterns, we developed a simple steady-state mathematical model. Analysis of plausible scenarios with this model confirmed that streams both have the capacity to remove allochthonous DIN over the plausible range of inputs, and that internal N sources are required to account for $\delta^{15}N$ signatures and observed DIN concentrations at stream outlets. Collectively, these data and modeling results demonstrate that N-fixation exerts substantial influence within and across these streams, and is presumably dependent upon interconnected organic matter reserves, mineralization rates, and geomorphology.

Keywords Cyanobacteria · Biofilm · C · N · P biogeochemistry · Hyporheic zone · Mineralization · MCM LTER

Responsible Editor :Thad Scott

Supplementary Information The online version contains supplementary material available at https://doi.org/10.1007/s10533-023-01069-0.

T. J. Kohler (✉) · J. G. Singley · A. N. Wlostowski · D. M. McKnight
Institute of Arctic and Alpine Research, University of Colorado, Boulder 80303, USA
e-mail: tyler.j.kohler@gmail.com

T. J. Kohler
Department of Ecology, Faculty of Science, Charles University, Viničná 7, Prague 2 128 44, Czechia

J. G. Singley
Department of Biology, Marine Biology, and Environmental Science, Roger Williams University, Bristol 02809, USA

A. N. Wlostowski
Boston Consulting Group, Boston, MA 02210, USA

D. M. McKnight
Department of Civil, Environmental and Architectural Engineering, University of Colorado, Boulder 80303, USA

Introduction

Nitrogen (N) fixation is one of the fundamental ways in which N can enter stream ecosystems. While the magnitude of this flux has been overshadowed by widespread N loading (Vitousek et al. 1997; Fowler et al. 2013), N-fixation may nonetheless be important to meeting nutrient budgets in N-limited systems globally, some of which include Earth's last remaining 'pristine' streams found in arid deserts, the poles, and alpine regions (Grimm and Petrone 1997; McKnight et al. 2007; Kunza and Hall 2014; Sohm et al. 2020; Bakker et al. 2022). Yet, even within these ecosystems, studies directly demonstrating the ecological influence of N-fixation are lacking, and the subject remains a considerable gap in the stream ecology literature (Marcarelli et al. 2008, 2022). One reason for this may be due to the majority of fixed N being assimilated into biomass (Marcarelli et al. 2008). Given that our understanding of the downstream fate of assimilated nutrients is currently limited to a few studies (e.g., O'Brien et al. 2012; Johnson et al. 2013), it is no surprise that we have a limited understanding of the role N-fixation plays in stream biogeochemistry.

Microbial activity in the hyporheic zone (HZ), likely manifesting as shallow benthic biolayers, is widely appreciated for performing the bulk of biogeochemical transformations in stream ecosystems. Organic matter (OM) enters the HZ where it is mineralized, and under anoxic conditions, can lead to N removal through denitrification. However, ammonium (NH_4^+) can also sorb to HZ sediments, and if redox conditions are appropriate, nitrification may also take place, transforming NH_4^+ to nitrate (NO_3^-). As a result, the HZ can also serve as a source of N at upwelling zones, making N available for microbial uptake downstream (e.g., Valett et al. 1994; Jones et al. 1995a, b). Although unquestionably important for processing OM (Findlay 1995; Boulton et al. 1998), most investigations of HZ transformations have been conducted over single stream reaches, largely due to logistical constraints and confounding factors that complicate greater study scales (e.g., riparian vegetation, tributaries, human activity, etc.). As a result, few studies have addressed questions related to HZ linkages at the landscape scale, although these scales are the most relevant for stream management and conservation (Krause et al. 2011).

The McMurdo Dry Valleys (MDVs) are the largest ice-free area of Antarctica, and here glacial melt creates extensive stream networks for several weeks of the austral summer (Fountain et al. 1999; Wlostowski et al. 2016). These streams are ideal for studying autochthonous OM cycling because they lack riparian vegetation (minimizing allochthonous inputs), lateral connectivity with the landscape (including groundwater due to extensive permafrost), and host negligible grazer biomass (McKnight et al. 1999). Yet, resident microbial life can be abundant, forming thick microbial mats ("mats" for brevity) on stream sediments and margins. Three mat types can be distinguished, which differ in color, streambed location, and dominant taxa (Kohler et al. 2015a; Van Horn et al. 2016). Specifically, "orange" mats cover the mainstem sediments and are chiefly comprised of filamentous cyanobacteria including genera *Leptolyngbya, Oscillatoria,* and *Phormidium*. "Green" mats are composed of chlorophytes and attach to large rocks. Lastly, "black" mats are formed by N-fixing *Nostoc* and are restricted to stream margins where they can form dense colonies (Fig. 1). All three mat types are perennial and grow at high abundances where geomorphological conditions are favorable (McKnight et al. 2007; Kohler et al. 2015a). Importantly, these mats (especially the black mats) are sources of coarse particulate organic material (CPOM) to the stream, with peaks in CPOM concentrations occurring on the rising limb of the daily flow pulse (Stanish 2011; Cullis et al. 2014).

In the MDVs, phosphorus (P) in streams is mostly derived from the weathering of apatite in the HZ (Bate et al. 2008; Heindel et al. 2018). Thus, P concentrations can increase downstream with other weathered solutes (Maurice et al. 2002; Gooseff et al. 2002). In contrast, the only abiotic input of N ultimately derives from atmospheric deposition of NO_3^-, which accumulates on, and is released from, source glaciers. Aside from this, all other N must originate from N-fixation and the mineralization of OM (Howard-Williams et al. 1989). The mats themselves act as nutrient sinks and readily take up added nutrients. Analysis of tracer experiments has shown that streams with greater mat coverage have greater nutrient uptake rates (e.g., Green Creek, Gooseff et al. 2004) than streams with low mat coverage (e.g., Huey Creek, Koch et al. 2010). As a result, streams with high mat coverage typically have lower nutrient

Fig. 1 *Nostoc*-based black mats as they appear in the field, with panel **a** showing their marginal position within a McMurdo Dry Valley stream, and panel **b** providing a detailed image

concentrations at their outlets than streams where mats are sparse (McKnight et al. 2004). Yet, measurable concentrations of nutrients are present at the outlets of all streams, despite high mat biomass that may be present for kilometers of stream length. It was thus hypothesized that glacier-derived N can be exhausted prior to reaching stream outlets given sufficient mat biomass and stream length, making downstream mat communities dependent upon mineralized N for their persistence (Howard-Williams et al. 1989; Kohler et al. 2018).

Nitrogen transformations in the HZ have been well-described in the MDVs (Gooseff et al. 2004; Koch et al. 2010), and coupled N-OM reactions in the HZ specifically are thought to be the mechanism by which sufficient nutrient regeneration takes place to facilitate downstream biomass (McKnight et al. 2004). In support of this, Kohler et al. (2018) utilized the distinctive stable isotopic signatures of different N sources in one MDV stream system (i.e. Relict Channel and Von Guerard) to show that the orange mats receive increasing proportions of *Nostoc*-derived N with greater distance downstream. Later, Heindel et al. (2021) used diatoms as a tracer to demonstrate that black mat biomass is transported in the stream and entrained in the HZ, and retained black mat biomass corresponded to greater NH_4^+ sorbed to sediments. Furthermore, Singley et al. (2021) found that HZ microbes are capable of nitrification and NO_3^- accumulates in the HZ. Yet, given that most of this research has been conducted in the same stream system (i.e., Von Guerard), the influence of these processes across MDV streams is not known, though necessary to resolve the importance of N-fixation for landscape-scale biogeochemistry in the MDVs and potentially streams in other settings as well.

We here ask two questions: First, how are $\delta^{15}N$ signatures of different mat types related to available N sources, specifically N-fixing black mats and DIN concentrations, across sites? Secondly, can mat $\delta^{15}N$ signatures be explained by their distance from the source glacier, approximating the degree of cumulative microbial processing? To answer these questions, we utilize the characteristic $\delta^{15}N$ signatures of different endmember sources in the MDV. Specifically, N originating through N-fixation should have $\delta^{15}N$ values near the atmospheric standard (~0‰), while nitrates in the MDV are characteristically depleted in $\delta^{15}N$ and range from − 26.2 to − 9.5‰ (Michalski et al. 2005). Based on the results from Kohler et al. (2018), we expect that black mats will have $\delta^{15}N$ values nearest the atmospheric standard across all sites, reflecting N-fixation as their primary N acquisition strategy. On the other hand, $\delta^{15}N$ signatures of

non-N-fixing orange and green mats should reflect overall N availability and possess intermediate signatures, being more $\delta^{15}N$ depleted where glacier-derived N is abundant, and more $\delta^{15}N$ enriched where *Nostoc*-derived N is the dominate N source (Peterson et al. 1997; Scott et al. 2007). Lastly, we predict that geomorphological conditions favoring high mat coverage, coupled with greater distance downstream, will enhance the effects of N scarcity and result in mat $\delta^{15}N$ signatures closer to the atmospheric standard (Fig. 2).

We address these questions using mat and water sample data taken from 22 MDV streams varying in biological, chemical, and physical conditions (Kohler and McKnight 2023). To complement these data, we further developed a tailored mathematical model to explore the plausible range (and interactions) of DIN sources and cycling parameters that can reproduce observed longitudinal $\delta^{15}N$ signatures of mats (Kohler 2018). By studying multiple streams in this model environment, we are able to assess the importance of in-stream N-fixation and autochthonous OM spiraling at the landscape scale. Given the widespread occurrence of *Nostoc* (Dodds et al. 1995), these results have potential implications, and applications, for other oligotrophic stream ecosystems worldwide.

Materials and methods

Site description

Taylor Valley (Fig. 3) is centrally located within the MDVs, and has been the subject of decades of stream ecosystem research thanks to its abundant streams, which are monitored for discharge, biomass, and chemistry by the McMurdo Long-Term Ecological Research (MCMLTER) program (http://mcm.lternet.edu). The region is ideal for testing basic controls on stream microbial mats because stream characteristics predictably shift from the Ross Sea coast (down-valley) to the Taylor Glacier (up-valley), and include a geochemical gradient that is reflected in long-term water chemistry of both the streams (Barrett et al. 2007; Welch et al. 2010) and the lakes they empty into (Priscu 1995; Foreman et al. 2004), with dissolved N:P ratios typically increasing up-valley towards the Taylor Glacier (Fig. 2).

Streams located down-valley near the Ross Sea coast, and especially in the Lake Fryxell Basin, generally tend to be longer, have a lower gradient, and have a stable stone pavement streambed. The valley narrows west towards Taylor Glacier, and streams here are shorter in length, have steeper banks and gradients, and are more likely to have fine, loose substrata (McKnight et al. 1999; Kohler et al. 2015a; Wlostowski et al. 2016). This gradient in geomorphology leads to dramatic differences in the abundance and coverage of microbial mats, with Fryxell Basin streams often harboring high coverages of orange and black mats, which is in sharp contrast to the Bonney and Hoare basins, where inhospitable conditions discourage dense mat growth (Kohler et al. 2015a).

The physical properties of MCM streams strongly influence hydrological and biogeochemical processes. For example, Leslie et al. (2017) showed that a shorter up-valley stream (i.e., Anderson Creek in the Lake Hoare Basin) presented a less well-developed HZ than a longer stream (i.e., Von Guerard in the Lake Fryxell Basin) where the HZ was much larger in size. This comparison may suggest that across the valley, shorter, higher gradient streams also may promote less weathering, exhibit lower uptake rates, and result in reduced OM processing than longer streams, potentially influencing the pool of available resources for biological uptake (and thus elemental and isotopic composition of microbial mats). Coupled with this (yet not totally independent), is the interacting effect of stream mat coverage in influencing nutrient uptake dynamics, as revealed through the results of the Green Creek versus Huey Creek tracer experiments (Gooseff et al. 2004; Koch et al. 2010), emphasizing that cumulative reach-level effects of the HZ could present themselves at landscape scales.

Sample collection

We surveyed 22 streams over Taylor Valley, the majority along established transects above their corresponding lake outlets (Table 1, Fig. 3). These transects vary by the width of a given stream, and are typically ~ 10 m in stream length. Mat abundance at these transects is related to geomorphology, and is generally representative for the stream as a whole. Both mat and summer streamflow characteristics are monitored by the MCMLTER (Kohler et al. 2015a; Wlostowski et al. 2016). All samples were taken from late

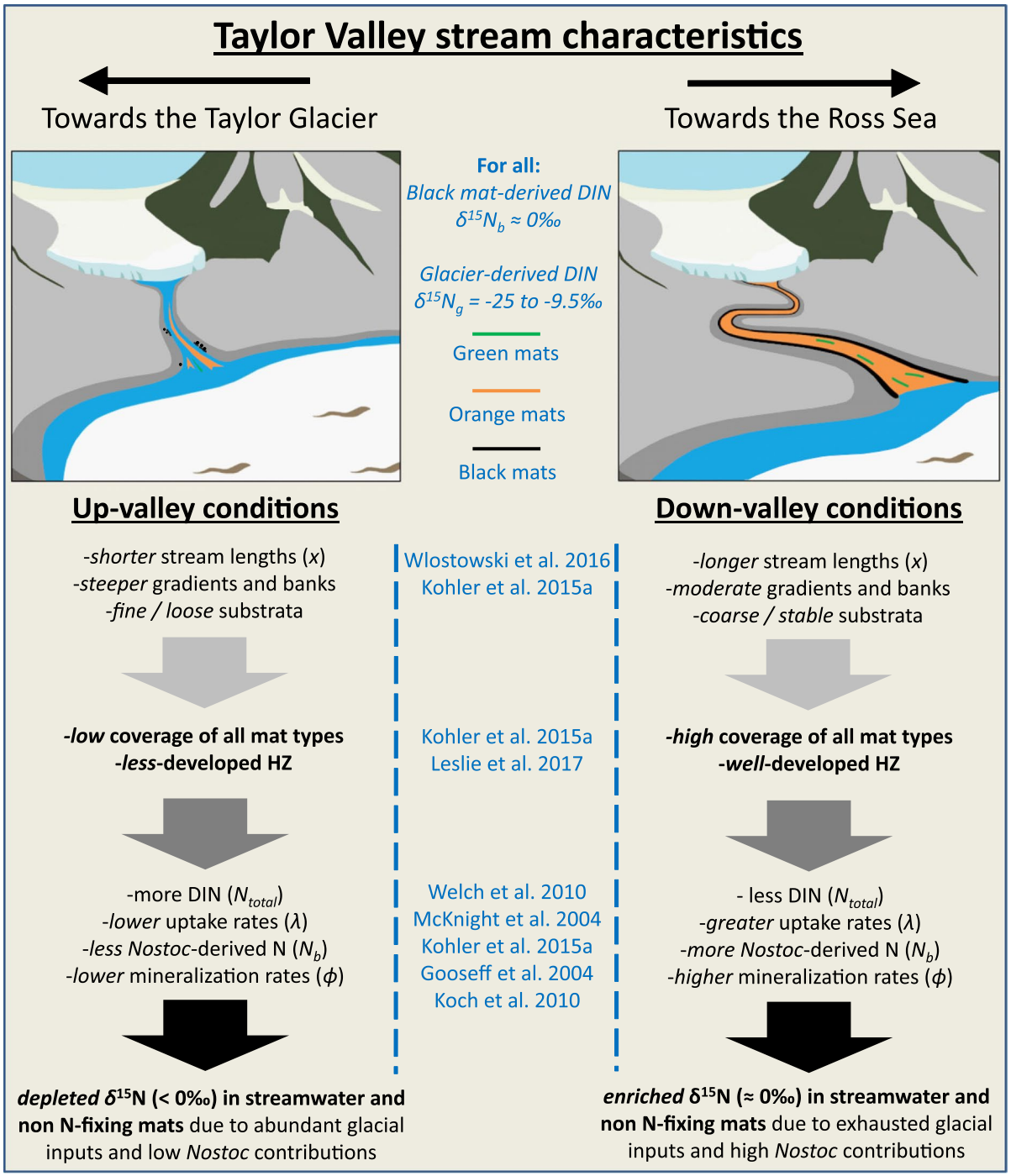

Fig. 2 Conceptual diagram illustrating the differences in stream characteristics from Taylor Glacier in the southwest (left) to the Ross Sea Coast in the northeast (right), with their anticipated consequences for $\delta^{15}N$ signatures

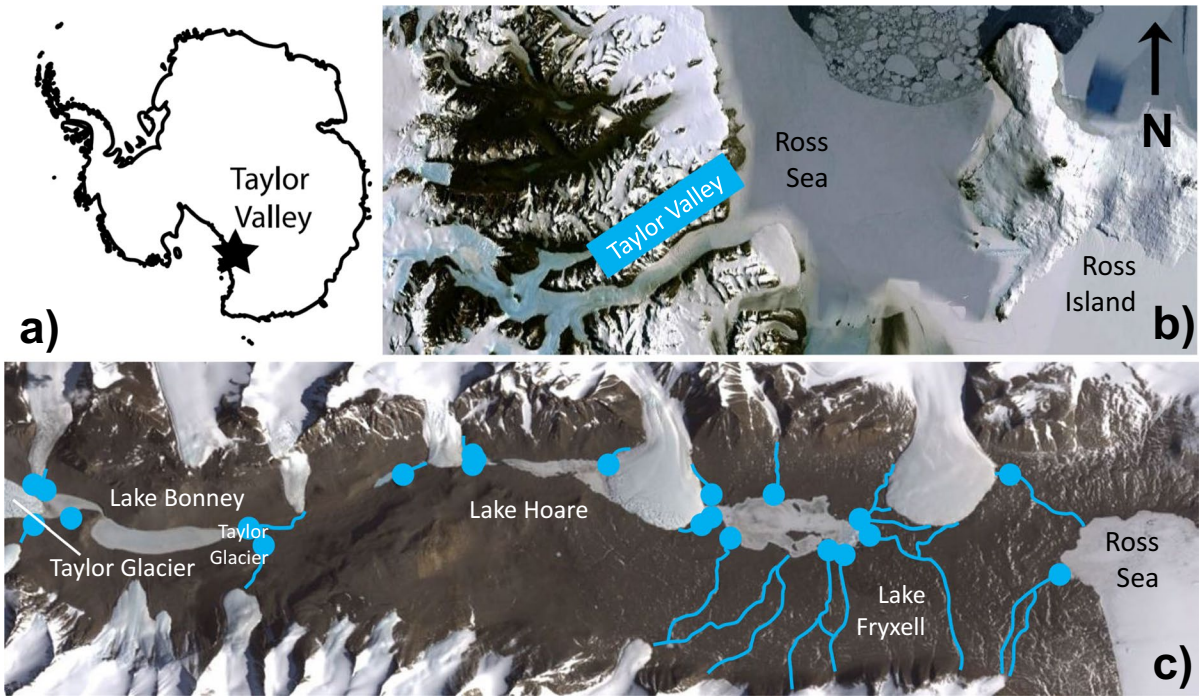

Fig. 3 Map of the study area, with **a** an inset of the Antarctic Continent indicating the location of Taylor Valley, and **b** a detail of the McMurdo Sound Region with Ross Island indicated at right and Taylor Valley highlighted at left. Panel **c** is a detail of Taylor Valley, with Taylor Glacier to the far left (southwest) and the Ross Sea coast to the right (northeast). Blue circles indicate the approximate location of samples taken at stream outlets, and the main channels of streams are superimposed with blue lines. Background images courtesy of the U.S. Geological Survey acquired via GoogleEarth©

December to late January within the 2011–2012 and 2012–2013 austral summers (Table 1). These summers were similar in discharge magnitude and duration (Kohler et al. 2015a, b), and samples analyzed from a given year were staggered spatially, such that there was a comparable geographic spread of sample collected across Taylor Valley from both years (thus, the 'year sampled' should not influence results, Table 1). From each transect, GPS coordinates were recorded and used to approximate the distance of a given sample to the source glacier using Google Earth©. Furthermore, given the well-described gradient of conditions from the Taylor Glacier (up-valley) to the Ross Sea coast (down-valley), the distance of a given site to the coast (near the New Harbor camp) was further approximated as an additional, 'comprehensive' variable.

The three different mat types create visually and compositionally distinct communities occupying different areas of the streambed (Alger et al. 1997; Kohler et al. 2015a), allowing for straightforward identification, differentiation, and sampling in the field. Given the inherent heterogeneity among streams, different mat types can either be found adjacent to each other or separated in space (e.g. different channels within the same stream). Furthermore, while 'mixed' communities can be present in areas of overlap near the stream margin (Kohler et al. 2015a, Fig. 1), care was taken to avoid sampling these assemblages to make subsequent interpretations as clear as possible. Accordingly, up to three different mat types—green, orange, and black—were sampled at each site if they were present within the transect. To account for natural heterogeneity, up to five replicates (overall average $n = \sim 3.5$) were taken across the transect for each mat type (depending on availability) for each analysis: ash-free dry mass (AFDM), chlorophyll-a (chla), and elemental and isotopic composition (C:N:P stoichiometry, and $\delta^{13}C$ and $\delta^{15}N$ isotopes). Sampling was executed by carefully lifting mats from substrata with a spatula, and cores taken with a brass cork borer (#13, 227 mm^2). Within 24 h,

Table 1 Taylor Valley stream transect name, outlet basin, GPS coordinates, mat types collected (G = green, O = orange, B = black), level of coverage, and austral summer samples for stoichiometry and isotopes were taken (January year)

Transect name	Drainage basin	Latitude (S)	Longitude (W)	Mat types	Mat coverage	January sampled
Wales Stream*	Ross Sea	− 77.57942	163.50575	O,B	Low	2013
Commonwealth Stream	Ross Sea	− 77.56361	163.38256	G,O,B	Low	2012
Aiken Creek	Fryxell	− 77.60153	163.29089	O,B	Low	2012
Lost Seal Stream	Fryxell	− 77.59595	163.24454	O	Low	2013
Von Guerard Stream Gage	Fryxell	− 77.60925	163.25408	G,O,B	High	2012–13
Harnish Creek	Fryxell	− 77.61221	163.23265	O,B	High	2012–13
Huey Creek	Fryxell	− 77.60231	163.12361	O,B	Low	2013
Delta Stream Gage	Fryxell	− 77.62533	163.10954	G,O,B	High	2012–13
Canada Stream Gage	Fryxell	− 77.61325	163.05322	G,O,B	High	2012
Green Creek	Fryxell	− 77.62441	163.05936	G,O,B	High	2012
Bowles Creek	Fryxell	− 77.62327	163.05776	G,O,B	High	2012
Andersen Creek	Hoare	− 77.62131	162.90698	O	Low	2013
House Stream	Hoare	− 77.64286	162.74227	O	Low	2012
McKay Creek	Hoare	− 77.64409	162.74612	O	Low	2012
Wharton Creek	Hoare	− 77.64465	162.74507	O,B	Low	2013
Popplewell Stream**	Mummy	− 77.65760	162.67897	O,B	High	2013
Priscu Stream	Bonney	− 77.69637	162.53614	O	low	2013
Bohner Stream	Bonney	− 77.69628	162.56392	G,O	Low	2012
Wormherder Creek	Bonney	− 77.72598	162.31551	O	Low	2012
Lyons Creek Tributary**	Bonney	− 77.72685	162.27992	O	Low	2013
Lawson Creek	Bonney	− 77.72036	162.26878	G,O,B	Low	2012
Little Sharpe Creek**	Bonney	− 77.72131	162.25880	O,B	Low	2013

Streams are listed roughly in order of increasing distance from the Ross Sea. (*) indicates only elemental composition was analyzed, (**) indicates unofficial stream name

all samples were dewatered onto Whatman® GF/F filters and frozen at − 20 ºC until later analysis.

Lastly, streamwater for nutrient chemistry analyses was collected opportunistically for each stream throughout the flow season, but always concurrently with mat sampling. This ranged from 1 to 10 samples for each stream transect per summer, with an average of 4.6 (median = 4.0) samples per stream in 2011–12 and an average of 4.9 (median 5.5) in 2012–13. Briefly, raw water was collected in triple-rinsed 250 mL Nalgene® bottles, filtered through glass-fiber filters, and frozen at the field station (Welch et al. 2010).

Laboratory analyses

Biomass was determined as in Kohler et al. (2015a) for chla and AFDM. Briefly, chla was quantified by extracting samples in 90% buffered acetone for 24 h (Welschmeyer 1994), measuring the concentration of chlorophyll-a in the supernatant on a Turner Designs 10-AU field fluorometer (Turner Designs, Sunnyvale, California), and scaling the result to the area of the brass cork borer used for sampling (final unit: µg chla cm^{-2}). AFDM subsamples were dried at 55 ºC for 24 h (or until a constant mass was achieved), weighed, burned at 450 ºC for 4 h, and reweighed to calculate mass loss following combustion (Steinman et al. 1996), which was similarly scaled to sample surface area (final unit: mg AFDM cm^{-2}). An autotrophic index (AI) was created by dividing chla values by their corresponding AFDM. All biomass analyses were performed in Crary Laboratory at McMurdo Station. In addition, coarse categorization of benthic coverage (i.e. 'low' and 'high') was made for each stream as in Alger et al. (1997), with less than 50% visual coverage qualifying as 'low coverage', and greater than 50% as 'high coverage'. In general, streams seldom approached '50%', and were mostly 'all or nothing' (particularly with regard to black

mats), creating little ambiguity between high and low coverage categories (Kohler et al. 2015a). Lastly, if no mats of a given mat type were present at the transect during the time of sampling (and thus could not be sampled), it was assigned a '0' rather than 'NA' in terms of its chla and AFDM.

The C:N:P and isotope subsamples were dried at 50–55ºC and ground to a powder. Prior to analysis, carbonates were removed from the C:N aliquot by fumigation (Hedges and Stern 1984) to prevent loss of acid-soluble carbon that may occur with rinsing (Harris et al. 2001). A second aliquot was analyzed without acidification in order to more accurately measure $\delta^{15}N$ values, which may slightly increase following fumigation (Harris et al. 2001). Percent C and N content was measured using a CE 1500 Elemental Analyzer (CE Instruments Ltd., Wigan, UK) and $\delta^{13}C$ and $\delta^{15}N$ isotope ratios were obtained with Finnigan-MAT Delta Plus XL mass spectrometer at the Center for Stable Isotope Biogeochemistry operated by the University of California, Berkeley. The %P aliquot was ashed in a muffle furnace at 500 ºC for 1 h, digested with 1N HCl, and analyzed as soluble reactive phosphorus (SRP) with a Lachat QuikChem 8500 Flow Injection Analyzer (Hach Company, Loveland, Colorado) by the Kiowa lab at the University of Colorado (Murphy and Riley 1962). A spinach standard (#1570a) was analyzed every ~ 10 samples to ensure method accuracy and digestion success. Resulting values were converted to molar C:N, C:P, and N:P ratios, and were used as a proxy to determine mat nutrient limitation through comparisons with the Redfield ratio (Redfield 1958).

Streamwater nutrient analyses were performed on either a Skalar San + + Continuous Flow Analyzer (2011–2012 summer) or a Lachat QuickChem Flow Injection Analyzer (2012–2013 summer) optimized for low concentrations (Welch et al. 2010). Dissolved inorganic nitrogen (DIN) was calculated as the sum of $N\text{-}NH_3^+$, $N\text{-}NO_2^-$, and $N\text{-}NO_3^-$. In general, NH_4^+ and NO_2^- were mostly low or undetectable. Detection limits for 2011–2012 nutrient data were 1 µg L^{-1} for N as $N\text{-}NO_2^-$ and NO_3^-, and 3 µg L^{-1} for P-SRP. For 2012–2013 nutrient data, detection limits were 1 µg L^{-1} for $N\text{-}NO_3^-$, 0.7 µg L^{-1} for $N\text{-}NO_2^-$, 5 µg L^{-1} for $N\text{-}NH_4^+$, and 0.6 µg L^{-1} for P-SRP. In cases where the measured concentrations of stream water nutrients were below detection limits, a value of half the respective detection limit was designated.

Stream water nutrient (DIN and SRP) concentrations are variable throughout the summer. Initial "first flow" concentrations can be orders of magnitudes higher in concentration than those later in the summer as the streambed is flushed, and greater discharge leads to nutrient dilution and uptake by reactivated mats (McKnight et al. 2007). Because of this, nutrient measurements represent "snapshots in time," while the algal mats themselves represent longer-term chemical "archives." Accordingly, we averaged all nutrient measurements from samples collected over a given summer to most accurately characterize individual transects. The results were in broad agreement with Welch et al. (2010), who showed that streamwater N:P ratios typically increase up-valley (away from the Ross Sea coast) using nearly two decades of monitored data. In streams with multiple gaging stations, only water chemistry from the 'mat transects' were used in calculations (i.e., where mats were sampled from).

Statistical analyses

Prior to univariate variable analyses, we conducted exploratory analyses to identify potential outliers and characterize data distributions (Zuur et al. 2009, 2010). Variables were averaged to create one value per mat type per stream (to reduce problems associated with uneven replication among streams), and data $\log_{10}(x)$-transformed to induce a normal distribution if necessary. Potential collinearity of explanatory variables was then assessed by pairs-plots and variance inflation factors. Due to the high collinearity found between explanatory variables (i.e. mat biomass, DIN, distance from glacier, distance from the coast), as well as assumed non-independence between these same variables, we opted to first create simple linear regression models (lm) to explain variability within individual parameters. Specifically, we tested how mat biomass, elemental composition, and isotopic signatures change as a function of black mat chla (proxy for N fixation), DIN concentration, their distance from the source glacier (a proxy for N uptake and OM processing), and the distance from the Ross Sea coast (comprehensive variable).

In order to find the most parsimonious combination of variables explaining $\delta^{15}N$ signatures for each mat type, we used Akaike information criterion corrected for small sample sizes (AICc, Burnham and

Anderson 2002) to compare different linear models including combinations of black mat chla, DIN, and distance from the source glacier ('distance from the coast' was not included because it theoretically already encompasses the former variables), along with a null model. Furthermore, differences between mat types (in terms of their biomass, elemental, and isotopic characteristics) were assessed with Tukey's Honest Significant Differences, and differences between high and low coverage streams assessed with Welch's t-test. Unless stated otherwise, all comparisons were performed individually between the different mat types (i.e. green, orange, black), and by using the R statistical environment (R Core Team 2022).

Modeling longitudinal DIN sourcing and cycling

We formalized the hypothesis that assimilatory uptake and coupled N-OM cycling results in a longitudinal shift in the predominant source of N in MDV streams into a set of coupled differential equations. This mathematical model simulates downstream changes in the relative fraction of glacier- and black mat-sourced inorganic N concentrations and the resulting bulk DIN isotopic composition. While the hydrology of MDV streams is highly dynamic, we chose to represent the system in steady state, again in accordance with the fact that algal mats themselves represent longer-term chemical "archives." For this model, Eq. 1 represents the spatial rate of change in isotopically depleted glacier-derived inorganic N. Equation 2 represents the black mat-derived inorganic N.

$$\frac{dN_g}{dx} = -\lambda\left(\frac{N_g^2}{N_g + N_b}\right) \tag{1}$$

$$\frac{dN_b}{dx} = \phi - \lambda\left(\frac{N_b^2}{N_g + N_b}\right) \tag{2}$$

Here, N_g is the concentration of glacier-derived inorganic N (μg L^{-1}), N_b is the concentration of black mat-derived inorganic N (μg L^{-1}), λ is the inorganic N uptake rate of orange mats (m^{-1}), ϕ is the flux of inorganic N from the HZ to the stream (μg L^{-1} m^{-1}) due to remineralization (combined with desorption following temporary storage by sediment), and x is the channel distance (m) measured from the glacier from which meltwater is supplied to the stream.

For any given channel distance, the $\delta^{15}N$ of DIN in stream water is calculated as:

$$\delta^{15}N_{x,pred} = \frac{\left(\delta^{15}N_g \cdot N_{g,x}\right) + \left(\delta^{15}N_b \cdot N_{b,x}\right)}{N_{g,x} + N_{b,x}} \tag{3}$$

where $\delta^{15}N_b$ is the isotopic signature of black mat matter, and $\delta^{15}N_g$ is the isotopic signature of glacier-derived DIN sources.

While the streams and biota of the MDVs have been studied extensively, the challenges associated with fieldwork in a polar desert environment limit the frequency and type of samples that have been collected, with most effort focused on stream outlets to lakes. Consequently, limited data are available on concurrent glacial meltwater DIN concentrations and isotopic signatures at both the head and outlets of streams for use in parameterizing the model. As such, we utilized the model to explore various potential N spiraling scenarios that could account for observed longitudinal mat isotopic patterns (e.g., Kohler et al. 2018), rather than determining a single best set of parameters. Specifically, we minimized an objective function for the residual sum of squares (Eq. 4) between model predictions of longitudinal DIN $\delta^{15}N$ and observed orange mat $\delta^{15}N$ composition for a single stream (Relict Channel, n = 14; Kohler 2018).

$$RSS = \sum\left(\delta^{15}N_{x,obs} - \delta^{15}N_{x,pred}\right)^2 \tag{4}$$

Using this approach, we fit the model to obtain λ and ϕ values for 25 independent simulations representing combinations of plausible values for the concentration and isotopic signature of glacial DIN inputs. We iteratively set the upstream boundary condition ($N_{g,x=0}$) to concentrations representing the 5th, 25th, 50th, 75th, and 95th-percentiles of observed DIN concentrations from 456 ice core samples for which DIN was detectable in MDV glacier ice core segments (Bergstrom and Gooseff 2021). We also varied $\delta^{15}N_g$ from –6‰, the most depleted orange mat sample observed in this stream, to –14‰, which we take as a conservative lower limit for steady state modeling at three times the standard deviation from the mean of $\delta^{15}N$ for orange mat samples collected across all sites reported here. It is unlikely that, on average, the $\delta^{15}N$ of glacial inputs is more depleted

than this value for the source glacier of this stream. Across all simulations, we held $\delta^{15}N_b$ equal to the atmospheric standard (0‰) to simulate black mat reliance on N fixation.

The resulting 25 model simulations generated longitudinal predictions of total DIN concentrations and the fractions therein from black mat and glacier sources, bulk $\delta^{15}N$ of the streamwater DIN and non-N-fixing orange mats, as well as uptake and remineralization/release coefficients (λ and ϕ). Again, due to the limited information for model parameterization, we limited our analysis to qualitative exploration of predicted longitudinal patterns and parameter relationships across the 25 simulations. Finally, we calculated differences in upstream and downstream boundary condition DIN concentrations to assess the magnitude of net DIN source or sink behavior required to generate the observed $\delta^{15}N$ patterns in orange mats under each glacial meltwater concentration and isotopic signature scenario.

Results

Differences between mat types

Black mats had the greatest mean biomass values (omitting zero values), averaging 21.63 (SD ± 8.25) mg AFDM cm^2 and 14.17 (±6.87) µg chla cm^2. Orange mats were intermediate, with 8.69 (±3.80) mg AFDM cm^2 and 7.37 (±4.70) µg chla cm^2, and green mats had the lowest average biomass, with 2.97 (±1.69) mg AFDM cm^2 and 3.76 (±2.59) µg chla cm^2. Comparisons with Tukey's test indicated that black mat AFDM and chla values were significantly greater than those for orange and green mats ($p < 0.002$ for all). Furthermore, orange mats had greater values than green mats in terms of AFDM ($p = 0.041$) but not in chla. Despite this, green mats had significantly greater AI (chla:AFDM) values (average 1.40 ± 0.78) than both orange mats (0.92 ± 0.41) and black mats (0.69 ± 0.29) ($p = 0.005$ and 0.048, respectively), but black and orange mat AI values were not significantly different.

Mat C:N:P stoichiometry was also measured to deduce possible nutrient limitation patterns. Observed C:N ratios were similar among mat types (black mean/SD = 10.55 ± 1.23; green = 9.35 ± 1.45; orange = 9.55 ± 0.98), and were greater than or equal to the Redfield Ratio (~7) in all streams. Orange mats had the lowest C:P ratios (though only significantly different from black mats, $p = 0.039$), and were consistently below Redfield Ratio (~106) averaging 49.10 (±30.00). The remaining mat types were above Redfield Ratio and had significantly greater C:P values than orange mats (both $p < 0.001$), with black mats averaging 137.84 (±59.81), and green mats 132.34 (SD ± 35.43). Finally, all mats were at or below Redfield Ratio for N:P (~16). Black mats had the greatest average at 15.89 (SD ± 6.96), a close match to the Redfield Ratio. Orange mats had the lowest N:P ratios averaging 5.67 (SD ± 3.73), while green mats averaged 14.44 (SD ± 5.27). Tukey comparisons revealed no significant different between N:P of black and green mats, but both these mat types had significantly greater N:P ratios than orange mats (both $p < 0.001$).

Mat types also differed in their isotopic ratios. Green mats had the lowest $\delta^{13}C$ values, averaging -24.34‰ (±3.40), and were significantly lower than in both orange and black mats (both $p < 0.001$). Meanwhile, orange and black mats were almost identical, measuring -17.31‰ (±4.05) and -17.38‰ (±1.76), respectively. Black mats were overall more enriched in their $\delta^{15}N$ signatures than other mat types, averaging -2.96‰ (±2.77). However, differences were only statistically different between black and orange mats ($p = 0.004$). The remaining two mat types were similar in their average $\delta^{15}N$ signatures, with -5.21‰ (±3.03) for green mats and -7.61‰ (±4.74) for orange mats.

Characteristics over Taylor Valley

Measured distances from transects to source glaciers significantly increased with distance down-valley, from the Taylor Glacier towards the Ross Sea (adj. $R^2 = 0.141$, df = 20, t = -2.108, $p = 0.048$). DIN concentrations significantly increased with increasing distance from the coast (adj. $R^2 = 0.144$, df = 20, t = 2.13, $p = 0.046$), while SRP significantly decreased over the same distance (adj. $R^2 = 0.141$, df = 20, t = − 2.11, $p = 0.047$). As a result, the streamwater molar N:P ratio significantly increased with distance from the coast (adj. $R^2 = 0.312$, df = 20, t = 3.241, $p = 0.004$). Most streamwater N:P values were above Redfield Ratio (~16) with an overall average of 49.62. In general, mat biomass measurements were poorly

related to the distance from the coast, and the only significant comparison belonged to black mats, whose chla (adj. $R^2 = 0.180$, df = 19, t = -2.32, p = 0.031) and AI (adj. $R^2 = 0.234$, df = 11, t = − 2.16, p = 0.053) significantly decreased away from the Ross Sea.

Over Taylor Valley, green mat C:N significantly decreased away from the coast (adj. $R^2 = 0.421$, df = 6, t = − 2.467, p = 0.049) whereas black mat C:N increased over the same distance (adj. $R^2 = 0.444$, df = 12, t = 3.371, p = 0.006). Meanwhile, there were no significant differences in orange mat C:N, or the molar C:P and N:P ratios of any mat type, with distance from the coast. DIN concentration had a significant, negative influence on orange mat C:N ratios (adj. R^2. = 0.138, df = 20, t = − 2.09, p = 0.050), but not on black or green mats. Similarly, increasing SRP concentrations reduced orange mat C:P values (adj. $R^2 = 0.178$, df = 20, t = − 2.353, p = 0.029), but there was no correlation with black or green mats. Neither DIN nor SRP alone significantly explained molar N:P of any mat type. Lastly, only orange mats showed patterns in $\delta^{13}C$ signatures, and increased away from the coast to Taylor Glacier (adj. $R^2 = 0.209$, df = 20, t = 2.556, p = 0.019).

The $\delta^{15}N$ signatures of all mat types were overall unrelated to their distance from the source glacier, and only black mats showed marginally-significant enrichment with increasing distance (adj. $R^2 = 0.221$, df = 12, t = 2.163, p = 0.051; Fig. 4). Additionally, increasing DIN concentrations was significantly associated with depletion in $\delta^{15}N$ signatures only for green mats (adj.$R^2 = 0.619$, df = 6, t = -3.516, p = 0.013), although this was marginally significant for orange mats (adj.$R^2 = 0.085$, df = 20, t = − 1.721, p = 0.101).

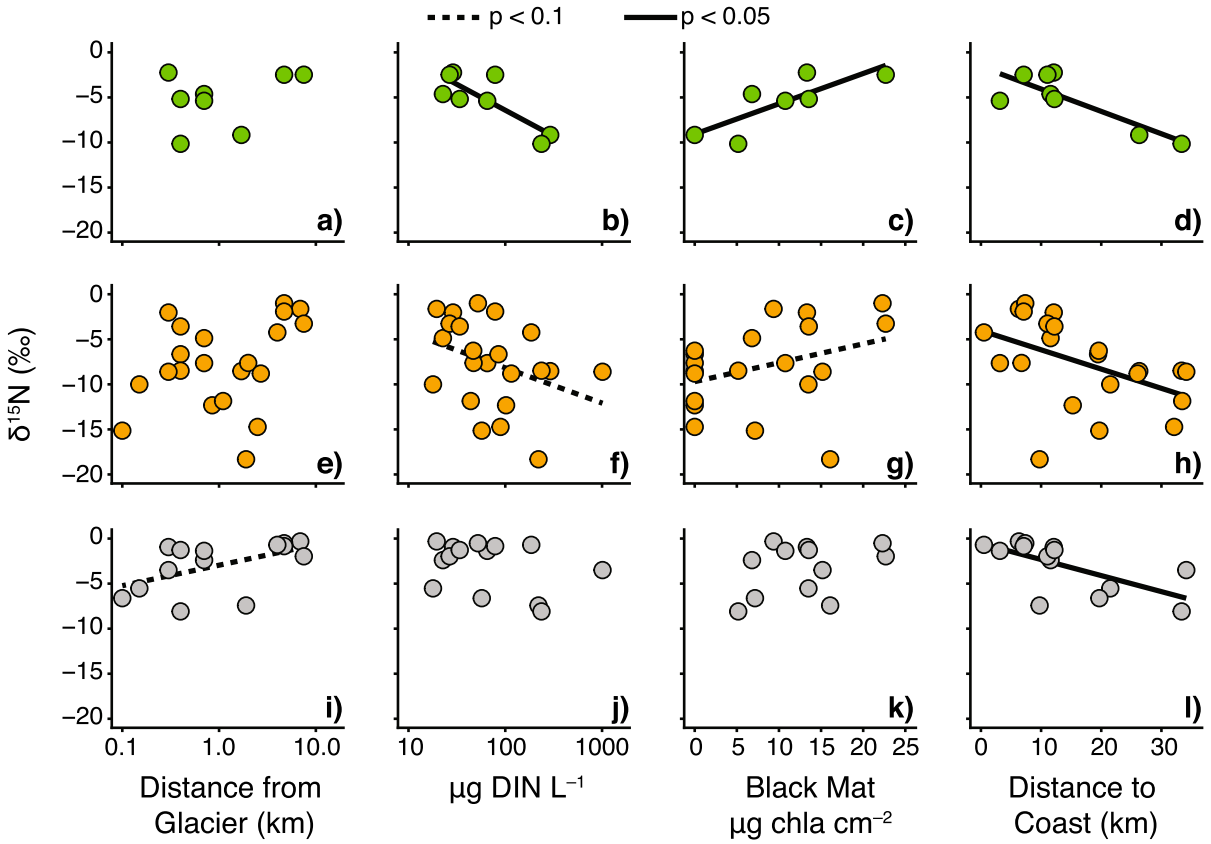

Fig. 4 $\delta^{15}N$ isotopic ratios for green (top row, a-d), orange (middle row, e–h), and black (bottom row, i-l) mats plotted against the distance from the source glacier (far left column), average transect DIN concentration (middle-left column), black mat chlorophyll-a (middle-right column), and the distance to the Ross Sea coast (far right column). Points are averages, and best-fit lines where present were calculated using least-squares linear regression. A solid line is given where p-values < 0.05, dashed lines for p-values between 0.05 and 0.10, and no line is given where p-values > 0.10

Furthermore, green (adj. $R^2 = 0.627$, df = 6, t = 3.572, p = 0.012) and (marginally) orange (adj. $R^2 = 0.102$, df = 19, t = 1.809, p = 0.086) mat $\delta^{15}N$ was significantly enriched as black mat chla increased (with black mat chla here used as a proxy for N-fixation), although there was no relationship with black mat $\delta^{15}N$ (Fig. 4). Lastly, the $\delta^{15}N$ of all mat types was compared with the distance to the coast as a 'composite' variable encapsulating gradients in DIN, black mat biomass, and distance from source glaciers. Orange (adj. $R^2 = 0.185$, t = 2.401, df = 20, p = 0.026), green (adj. $R^2 = 0.632$, df = 6, t = 3.606, p = 0.011) and black (adj.$R^2 = 0.383$, df = 12, t = − 3.010, p = 0.011) mats were all significantly more depleted in their $\delta^{15}N$ signatures as transect distance from the coast increased (Fig. 4).

In addition to these comparisons, we also tested for differences among streams with high and low coverages of mats. In all, there were 15 low-coverage and 7 high-coverage transects sampled (Table 1). High coverage streams had significantly lower DIN concentrations than low coverage streams (high coverage mean = 37.2 µg L^{-1}, low coverage mean = 174.4 µg L^{-1}; Welch's t-test, t = − 3.62, df = 19.58, p = 0.002). While SRP also showed lower concentrations in high versus low coverage streams (5.15 versus 17.04 µg L^{-1}, respectively), this difference was not statistically significant. Furthermore, none of C:N, C:P, N:P, nor $\delta^{13}C$ were significantly different between high and low coverage streams for orange and black mat types (green were not tested due to low sample size). However, orange mat $\delta^{15}N$ signatures were significantly greater in high coverage streams (t = 3.48, df = 16.70, p = 0.003, Fig. 5), though there was no statistical difference in black mat $\delta^{15}N$ between stream types.

Lastly, we also compared and ranked different linear models to find the most parsimonious combination of variables explaining mat $\delta^{15}N$ (Table 2). We found that black mat chla was present in the highest-ranking model for all three mat types, indicating an overall high level of influence. More specifically, the best model for green mats was black mat chla alone, garnering 44% of the weight, followed by DIN alone, which accounted for another 40%. For orange mats, the top model included both DIN and black mat chla (39% of the weight), followed by black mat chla alone (34%), and then by distance to the glacier combined with black mat chla (11%). Lastly, for black mats, the best model again was black mat chla alone (38% of the weight), followed by the combination of DIN and black mat chla (28%), and then by distance to the glacier (10%).

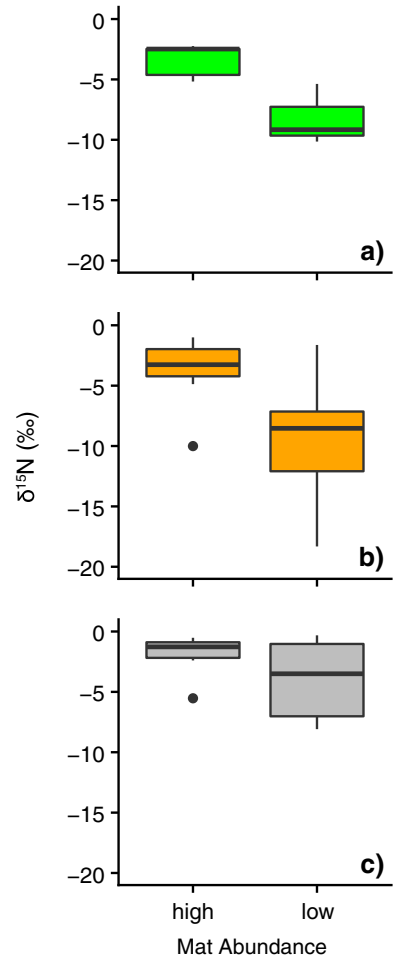

Fig. 5 Boxplots of $\delta^{15}N$ isotopic ratios for green (top, **a**), orange (middle, **b**), and black (bottom, **c**) mats for high and low coverage stream transects. High and low coverage designations are taken from Alger et al. (1997) and Kohler et al. (2015a), with remaining designations reported in Table 1

Modeled longitudinal DIN sourcing and cycling

The optimized parameters for DIN uptake (λ) and black mat-derived N release (ϕ) for our steady state model closely replicated the observed longitudinal orange mat $\delta^{15}N$ composition patterns in the Relict Channel for all upstream boundary concentrations and N source isotopic composition combinations that we simulated. Specifically, the average root mean

Table 2 AIC*c* output for linear models describing green, orange, and black mat $\delta^{15}N$ signatures. Models with weights greater than or equal to 10% are shown in bold

Mat type	Parameter	k	AICc	ΔAICc	AICc Wt	Cum. Wt	LL
Green	**B_chla**	**3**	**42.23**	**0**	**0.44**	**0.44**	**– 15.12**
	DIN	**3**	**42.40**	**0.17**	**0.40**	**0.85**	**– 15.2**
	null	2	45.75	3.52	0.08	0.92	– 19.67
	DIN + B_chla	4	46.78	4.55	0.05	0.97	– 12.72
	transect + DIN	4	48.32	6.09	0.02	0.99	– 13.49
	transect	3	50.43	8.20	0.01	1	– 19.21
	transect + B_chla	4	51.44	9.21	0	1	– 15.05
	transect + DIN + B_chla	5	63.59	21.36	0	1	– 11.8
Orange	**DIN + B_chla**	**4**	**128.19**	**0**	**0.39**	**0.39**	**– 58.85**
	B_chla	**3**	**128.48**	**0.28**	**0.34**	**0.73**	**– 60.53**
	transect + B_chla	**4**	**130.75**	**2.55**	**0.11**	**0.84**	**– 60.12**
	transect + DIN + B_chla	**5**	**130.78**	**2.59**	**0.11**	**0.94**	**– 58.39**
	DIN	3	134.16	5.97	0.02	0.96	– 63.41
	null	2	134.50	6.30	0.02	0.98	– 64.93
	transect + DIN	4	135.25	7.06	0.01	0.99	– 62.45
	transect	3	135.60	7.40	0.01	1	– 64.13
Black	**B_chla**	**3**	**68.36**	**0**	**0.38**	**0.38**	**– 29.85**
	DIN + B_chla	**4**	**68.95**	**0.60**	**0.28**	**0.66**	**– 27.98**
	transect	**3**	**71.02**	**2.66**	**0.10**	**0.76**	**– 31.31**
	transect + B_chla	4	71.15	2.79	0.09	0.86	– 29.07
	null	2	72.32	3.96	0.05	0.91	– 33.62
	transect + DIN	4	73.02	4.66	0.04	0.95	– 30.29
	transect + DIN + B_chla	5	73.48	5.12	0.03	0.97	– 27.45
	DIN	3	73.77	5.42	0.03	1	– 32.69

AIC indicates Akaike's Information Criterion, k indicates the number of parameters (including intercept and error terms), ΔAIC*c* is the difference between the AIC*c* value and the lowest AIC*c* value, AIC*c*Wt is the relative likelihood that the model is the best approximating model, Cum.Wt is the cumulative weight, and LL is log likelihood. Variable abbreviations: "DIN" = dissolved inorganic nitrogen, "transect" = distance of a transect from the source glacier, and "B_chla" = black mat chlorophyll-a concentration at the given transect

square deviation between observed and predicted longitudinal $\delta^{15}N$ across the 25 fitted models was 1.1‰ (±0.7). The results for the scenarios based on the observed median $N_{g,x=0}$ concentration – the most likely condition – are presented in Fig. 6 (with N_g indicating the concentration of glacier-derived DIN), while the corresponding longitudinal results for the scenarios based on the 5th, 25th, 75th, and 95th percentile $N_{g,x=0}$ concentrations are presented in the supplemental material, Fig. S1–4). For the median $N_{g,x=0}$ cases, the rise of orange mat $\delta^{15}N$ to near 0‰ with increasing channel distance (Fig. 6a–e) is dependent on rapid and complete removal of glacier-derived DIN in the upper reaches of the modeled channel (Fig. 6f–j) while black mat-derived DIN increases rapidly and then stabilizes in all scenarios. Generally, total DIN concentrations decline and eventually stabilize towards the stream outlet, though scenarios with more isotopically depleted glacier-derived DIN also predict longitudinally increasing concentrations due to a more rapid rise in the black mat-derived DIN fraction to reproduce the observed total DIN $\delta^{15}N$ values. As outlet concentrations were not constrained in the model optimization, we note that simulations with more depleted glacial sources predict higher outlet DIN concentrations, though all simulations predict concentrations within the range observed at stream outlets. Importantly, this variation in predicted outlet concentrations is a mathematical effect of mixing various endmember signatures to achieve the same bulk isotopic composition in stream water and is not suggestive of preferential uptake in this highly oligotrophic system.

Across all the scenarios, the fitted uptake coefficient (λ) varied by a factor of just over two (0.02–0.05 m^{-1}), while the black mat-derived DIN release coefficient (ϕ) varied much more widely (0.06–3 μg L^{-1} m^{-1}). We found that for this model formulation, ϕ was linearly related to the glacial source $\delta^{15}N$, with the slope of the relationship approaching zero as the concentration of glacial inputs declined (Fig. 7a). We observed that λ also

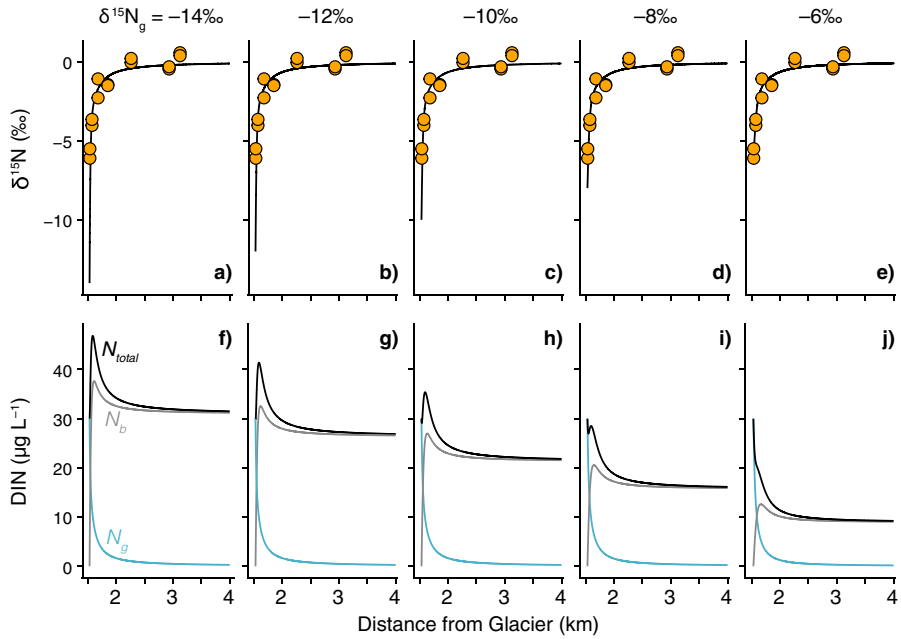

Fig. 6 Observed longitudinal trends in $\delta^{15}N$ of orange mats in the Relict Channel with model predictions of DIN isotopic composition (top row, a-e) and source fractions (bottom row, f-j) across a range of glacial-derived DIN input signatures (columns). Each simulation utilized the median DIN concentration from ice cores as an upstream boundary condition. Similar results from simulations utilizing the 5th, 25th, 75th, and 95th-percentile observed glacial DIN concentrations are provided in Supplemental Fig. S1-4. N_{total} indicates the total concentration of DIN, N_b the concentration of black mat-derived DIN, and N_g the concentration of glacier-derived DIN (all in μg L^{-1})

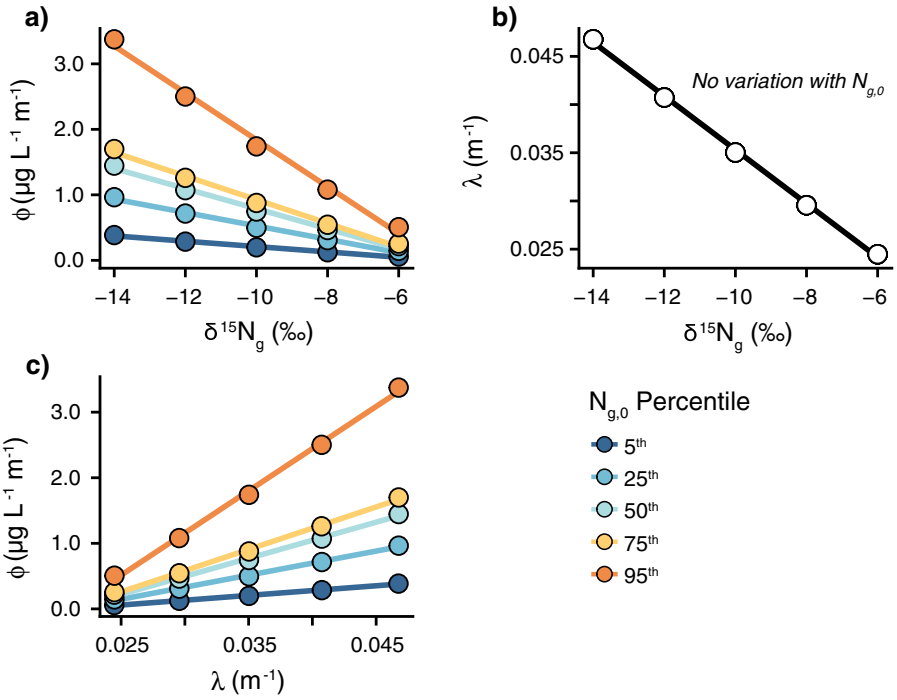

Fig. 7 Model parameter relationships across the 25 simulations fitted to Relict Channel orange mat isotopic composition. **a** $\delta^{15}N$ of glacial-derived DIN inputs versus fitted autochthonous N release coefficient (ϕ) with variations in glacial meltwater DIN concentrations. **b** $\delta^{15}N$ of glacial-derived DIN inputs versus fitted uptake coefficient (λ). **c** Relationships between ϕ and λ with variations in glacial meltwater DIN concentrations

declined linearly with $\delta^{15}N_g$, though this relationship was notably not dependent on the concentration of glacial inputs (Fig. 7b). As expected, these combined relationships predict that higher orange mat DIN uptake coefficients must be associated with proportionally larger increases in black mat-derived DIN release rates, with exact relationship slopes dependent on the concentration of DIN in glacial meltwater (Fig. 7c).

Finally, the model predicts that while the predominant source of available DIN shifts from glacial meltwater to black mats with increasing channel distance, reproducing orange mat isotopic patterns requires that the streams function as net DIN sinks under most scenarios (Fig. 8). Only in cases with the most extremely depleted $\delta^{15}N$ values (i.e., -14‰) for glacier-derived DIN, does the model predict that the streams function as net DIN sources to reproduce orange mat signatures. Across all other scenarios, the model predicts that the stream must function as a stronger DIN sink (up to ~ 2/3 reduction in concentrations) when glacial $\delta^{15}N$ values decrease. That is, reproducing the longitudinal signature of orange mats requires smaller releases of black mat-derived DIN in scenarios for which the glacial DIN source itself has an isotopic signature closer to the atmospheric standard.

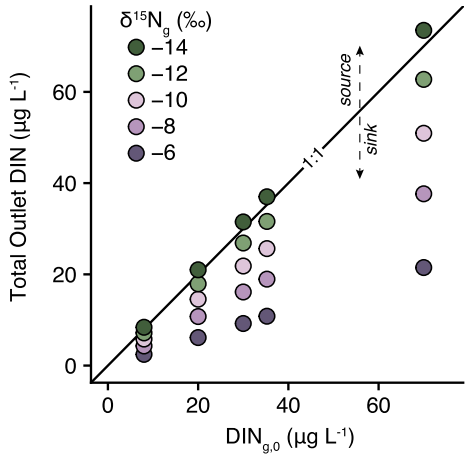

Fig. 8 Modeled steady-state DIN inputs from glacial meltwater versus outlet (x = 4000 m) for the Relict Channel across all model simulations with 1:1 reference line distinguishing net DIN source or sink behavior

Discussion

Through field observations and modeling, we here provide evidence that N-fixation represents a substantial contribution to MDV stream N budgets at the landscape scale. Across MDV streams, black mat biomass had a C:N ratio matching the Redfield ratio, and greater average $\delta^{15}N$ signatures than other mat types. Overall, $\delta^{15}N$ signatures of orange and green mats increased with greater black mat chla and lower DIN concentrations – conditions exemplified in down-valley streams near the coast. Furthermore, orange mats (but not black) were significantly more enriched in $\delta^{15}N$ when coming from streams with high mat coverage (equating to lower DIN concentrations but greater *Nostoc* biomass), yet were not more enriched than the atmospheric standard ($\delta^{15}N \approx 0‰$). In addition to these findings, a steady state model revealed that N-fixation is required to account for observed longitudinal $\delta^{15}N$ signatures and DIN concentrations at stream outlets. Collectively, these results demonstrate the ecological importance of N-fixation to MDV streams, and exemplify the connectivity between hydrologic and geomorphic processes, biogeochemistry, and different biological compartments at the landscape scale.

N-fixation in the MDV

Given the fundamental importance of N-fixation and the common occurrence of *Nostoc* in temperate streams (Dodds et al. 1995), the limited exploration of this topic is remarkable (Marcarelli et al. 2008, 2022). Even in MDV streams, N-fixation was historically assumed to be of limited importance to N budgets, despite visually high coverages of black *Nostoc* mats. Yet, the molecular machinery for N-fixation in black mats is common across the MDV landscape (Coyne et al. 2020; Zoumplis et al. 2023), and several recent studies have shown N-fixation rates to be relatively high and comparable to warmer systems at lower latitudes (McKnight et al. 2007; Sohm et al. 2020). Nonetheless, N-fixation rates alone are not sufficient for estimating the contribution of N-fixation at the landscape scale, because like with MDV streamwater nutrient chemistry, they are but a snapshot in time. Thus, another line of evidence for the importance of N-fixation in these systems are mat $\delta^{15}N$

signatures because they account for the cumulative, long-term importance of this N source.

Recently, we found evidence that N-fixation contributes to nutrient budgets along the longitudinal gradient of one stream system (Kohler et al. 2018; Heindel et al. 2021; Singley et al. 2021), which led to our hypothesis that N-fixation is influential to streams across the entire MDV landscape. We predicted that black mat $\delta^{15}N$ signatures will be consistently the most enriched and near the atmospheric standard, reflecting N-fixation (Peterson and Fry 1987; Michener and Lajtha 2007). Because orange and green mats presumably fix less N than black mats, their isotopic compositions should largely reflect what is available for uptake. As a result, we hypothesized their signatures should be more variable than black mats across sites, reflecting the more depleted glacier-derived N when it is available, and the more enriched *Nostoc*–derived N when black mat biomass is high and DIN is low (Michalski et al. 2005; Scott et al. 2007).

Overall, our hypotheses were supported in that mat $\delta^{15}N$ signatures were more likely to be enriched where DIN concentrations were lower and *Nostoc* biomass greater. However, while *Nostoc* overall had more enriched $\delta^{15}N$ signatures, and signatures indicative of N-fixation notably in the high coverage / N-limited streams of the Fryxell Basin, they also exhibited $\delta^{15}N$ depletion in up-valley streams (characterized by low coverage/high DIN), suggesting uptake of glacier-derived DIN along with other mat types. This scenario was exemplified in Huey Creek, which was an outlier in the Fryxell Basin. Huey Creek drains a snowfield in the Asgard Range, and mats are sparse due to frequent flooding, high sediment loads, and unstable substrata (Runkel et al. 1998; Koch et al. 2010). Here, all mat types, including black mats, were anomalously depleted, indicating assimilated N derived from the snowfield rather than N-fixation. Similarly telling are the $\delta^{15}N$ signatures of orange and black mats from Lawson Creek in the Bonney Basin (up-valley near Taylor Glacier), which were ~ − 8‰ for both mat types.

Given that water availability (and by extension, DIN) for black mats is variable due their location at stream margins, the ability for black mats to alternate nutrient pathways is an asset energetically (Dodds et al. 1995). Where N is abundant, black mats can assimilate N at low metabolic cost (fixation may even cease), resulting in $\delta^{15}N$ depletion. Alternatively, these more depleted $\delta^{15}N$ signatures may also indicate changes in species composition within the black mats. While morphological investigation through microscopy indicates that most of the black mat biomass is comprised of *Nostoc* with taxa from other groups occasionally present (e.g. Alger et al. 1997), recent molecular investigations have shown black mats to be more compositionally diverse (Van Horn et al. 2016; Zoumplis et al. 2023), though still largely dominated by *Nostoc*. Thus, it could be that changes in black mat isotopic signatures could be related, at least in part, to community shifts within the mat, though this requires further investigation.

In addition, depletion/enrichment patterns among mats may be partially due to the degree of processing taking place from source glaciers to corresponding outlets. 'Nutrient spiraling' conceptualizes how nutrients cycle within streams, and a 'spiral' begins with an element (such as N) traveling through the water column in an inorganic form, followed by its incorporation into biota, and is completed by its release back into the water column in an inorganic form, all while traveling downstream (Newbold et al. 1981). In low coverage streams, the length required for N to complete a spiral is longer than in high coverage streams because DIN concentrations will be relatively high and uptake rates low. Thus, from glacier to mouth, each atom of N is likely to be biogeochemically transformed fewer times than an atom of N released into a high coverage stream, and these differences likely intensify as stream length increases, such as in those near the coast. Biological processes such as nitrification and denitrification discriminate against the heavy N species (Lehmann et al 2003; Michener and Lajtha 2007), preferentially removing the lighter isotope (Montoya and McCarthy 1995). Because of these small fractionations with each biological transformation, some degree of $\delta^{15}N$ enrichment might be observed in mats with greater cumulative processing due to this mechanism alone.

However, we argue that differences in N sources are likely more influential in determining the final isotopic signature of mats than repeated processing. Firstly, mat uptake and assimilation of NO_3^- has been shown to be orders of magnitude higher than HZ denitrification and dissimilatory reduction (Gooseff et al. 2004; McKnight et al. 2004). Secondly, if nutrient transformations were a highly influential mechanism

for N isotopic signatures in this system, we would expect to see $\delta^{15}N$ values occasionally surpassing the atmospheric standard of ~ 0‰, especially in longer streams. Yet, both in this study and its predecessor (showing longitudinal trends in Von Guerard, one of the MDV's longest streams; Kohler et al. 2018), this proved not to be the case. In fact, the $\delta^{15}N$ signatures of mats from the outlets of longer streams (e.g. Delta and Von Guerard) were comparable with the samples from the outlets of some shorter streams (e.g. Bowles and Green), with black mat signatures near ~ 0‰ and other mat types slightly less, but none substantially above 0‰. This indicates that the enrichment effect is primarily from the uptake of *Nostoc*–derived N that is re-mobilized in the HZ through degradation of entrained black mat-derived CPOM carried by the streams on a daily basis (Cullis et al 2014).

Overall, we found limited significant relationships with mat $\delta^{15}N$ signatures and the distance from the source glacier. Given our rather broad range of distances across sites (ranging from 0.05 to 7.5 km, with median = 0.98 km), we expected to find progressive enrichment across sites with greater distances downstream. For example, in the Relict Channel (Kohler et al. 2018), the $\delta^{15}N$ signatures of orange mats rose rapidly over a distance of ~ 1 km, and converged with those of black mats at approximately 2 km downstream, and remained approximately consistent for the remaining ~ 2.5 km. Yet, the point of this isotopic shift in the Relict Channel coincided with a loss of slope, channel widening, and an increase in biomass, following the emergence of the stream from the Kukri Hills. With this in mind, it seems that these isotopic shifts can be punctuated (if they take place at all), and likely stream-specific, being dependent upon glacier- and black mat-derived N availability at a given transect, as well as the geomorphology and cumulative upstream processes. Therefore, it may be difficult to predict mat $\delta^{15}N$ signatures across diverse sites based on the distance from the glacier alone.

Insights from the exploratory model

Our highly simplified steady-state model agrees with prior interpretations (e.g., Kohler et al. 2018) of longitudinal mat isotopic patterns resulting from the rapid removal of isotopically depleted glacier-derived DIN and increasing reliance on N sourced from autochthonous black mat N fixation. Our range of exploratory simulations demonstrates that (provided DIN uptake and release processes are tightly coupled) there are many plausible combinations of source signatures, concentrations, and biogeochemical dynamics that can account for the observed relationships between stream length and mat isotopic signatures – but all demonstrate that in-stream N fixation facilitates mat biomass and reliance on this autochthonous source of N increases with stream length. Moreover, except for scenarios involving the most extremely depleted glacial DIN sources, our models generally agree with the typical characterization of MDV streams as DIN sinks (e.g., Gooseff et al. 2004; McKnight et al. 2004; Dubnick et al. 2017) and highlight that efficient net retention of N is maintained along with substantial biotic spiraling and physical storage within the HZ (Singley et al. 2021, 2023).

We acknowledge that our model results should be interpreted carefully, and primarily qualitatively, given known limitations of this simple formulation. Namely, we do not account for the substantial diel and seasonal variations in flow conditions characteristic of MDV streams that influence CPOM transport or known temporal variations in nutrient supply (Cullis et al. 2014; Wlostowski et al 2016). However, we argue that our steady state formulation is likely still valid given that mat $\delta^{15}N$ signatures probably reflect a running average of available DIN compositions, rather than singular moments of uptake. On the other hand, our model does not account for flexible N acquisition strategies of black mats suggested by the new data presented here (e.g., Fig. 4i,l). Therefore, longitudinal predictions of the fraction of DIN derived from black mats might be more accurately interpreted as the fraction supplied only by black mats that have relied on N fixation. Our model also does not differentiate immediate remineralization of freshly mobilized autochthonous OM from remineralization of stored OM in the HZ, the latter of which is the largest pool of N in some MDV streams (Singley et al. 2021, 2023). Additionally, *Nostoc* is known to be "leaky" and releases both DIN and DON (Glibert and Bronk 1994; Mayland et al. 1966), particularly when N fixation is elevated (Barr 1999). Given that orange mats can presumably process and assimilate organic N (Howard-Williams et al. 1989; Zoumplis et al. 2023), in-stream N fixation may also subsidize downstream mats through pathways that do not require remineralization of OM in the HZ.

Despite these caveats, this simple exploratory modeling exercise provides insights to guide future studies of coupled N fixation and autochthonous OM cycling in MDV streams. Principally, inferring coupled N-OM spiraling parameters (i.e., uptake and release coefficients) requires further characterization of N source signatures and concentrations, not merely longitudinal mat $\delta^{15}N$ patterns. Yet, doing so is further complicated by the fact that N cycling can occur in glacial melt as it is transported in supraglacial streams in the MDV (Bergstrom et al. 2020), which may impart greater variation in both N concentrations and isotopic composition than is currently assumed for this source.

Implications for the future

By utilizing simplified stream systems, we here demonstrate the importance of N-fixation in meeting nutrient demands across MDV streams. In this region, recent increases in streamflow have accompanied increases in black mat biomass over the last decades (in contrast to a decrease in black mat biomass observed during a relatively cool period in the 1990's; Kohler et al. 2015a; Gooseff et al. 2017). If black mat N additions fuel in-stream biomass, this may help explain why *Nostoc* was able to recover from the effects of an anomalously high melt season in 2002 (i.e. the 'flood year') more rapidly than orange mats, with black mats recovering almost immediately, while orange mats experienced a 5-year lag (Gooseff et al. 2017). Previously, black mats were shown to be less responsive to historical flow conditions than other mat types (i.e., orange and green), which was assumed to be because of their marginal position in the stream, which might reduce instances of scour (Kohler et al. 2015a). However, given results in Stanish (2011), Kohler et al. (2018), and Heindel et al. (2021), all of whom found black mat biomass to be disproportionately represented either in the HZ or in CPOM, the opposite might actually be true: black mats are probably more prone to being dislodged, and may instead correlate poorly with hydrological variables because they face regular disturbance (i.e., daily with the flood pulse), whereas other mat types are more resistant to these regular fluctuations, and therefore more responsive to larger scale disruptions.

Future changes to dissolved N concentrations brought forth due to changes in the abundance of black mats could also result in biomass and community shifts, as shown previously with nutrient additions in N-limited Fryxell Basin streams (Kohler et al. 2016). As a result, *Nostoc* may play a disproportionate role in regulating the biomass, diversity, and nutrient biogeochemistry of streams, as well as potentially regulate the content of water that enters at lake margins. Furthermore, given the sparse distribution of OM across the MDV landscape, the redistribution of biomass from 'hotspots' such as streams and lake margins may be critical in fueling heterotrophic processes in soils, as well as other habitat types such as cryoconite (Barrett et al. 2007). Thus, N-fixation in MDV streams may have landscape implications that transcends stream habitats.

Although representative of freshwater streams in the desert oases around the coast of Antarctica, the MDV are a unique locality given their absence of terrestrial vegetation and anthropogenic N-inputs. While the occurrence of *Nostoc* mats at stream margins is also common in temperate regions, it is possible that this combination of N-fixation and HZ exchange may only be a *dominant* process in some oligotrophic settings globally. Recent reviews have suggested that N-limitation may be widespread among other glacier-fed ecosystems (Ren et al. 2019; Elser et al. 2020) as well as in some non-glacial streams across the arctic (Myrstener et al. 2018), and increasing temperatures have been shown to stimulate N-fixation rates (Welter et al. 2015). Thus, the importance of N-fixation to these threatened habitat types may be underestimated (not to mention other oligotrophic and/or high-P environments globally), and is likely to evolve with ongoing climate change.

Conclusions

This study provides one of the best examples to date of the potential importance of N-fixation and the cumulative effects of OM processing by illustrating their influence on the $\delta^{15}N$ composition of stream microbial mats at the landscape scale. Indeed, it is possible that the role of N-fixation to streams elsewhere has been underestimated given that mass-balance calculations may not reflect the true importance of this flux given the cumulative nature of mineralization and uptake processes. We therefore encourage future investigators to consider the importance

and cumulative effects of N-fixation outside pristine, N-limited sites, and especially across landscapes.

Acknowledgements We thank Chris Jaros, Jeb Barrett, Dave Van Horn, Jenny Erwin, Samantha Weintraub, Tim Seastedt, Kathy Welch, the University of California Berkeley Center for Stable Isotope Biogeochemistry, the University of Colorado Kiowa Lab, and our friends at Crary Laboratory and McMurdo Station for help with fieldwork, laboratory assistance, and critical comments. Lastly, we thank Dr. Thad Scott and an anonymous reviewer for their comments, which greatly improved the manuscript.

Author contributions TJK and DMM designed the experiment and conducted the fieldwork. TJK, JGS, ANW, and DMM analyzed the data, performed the modelling, and interpreted the results. TJK wrote the paper with editorial input from all authors.

Funding Funding was provided by the MCMLTER (OPP-1115245). TJK was further supported by the Charles University project PRIMUS/22/SCI/001 and by the Charles University Research Centre program no. 204069.

Data availability All data presented in this study are archived in the Environmental Data Initiative (EDI) Data Repository, https://doi.org/10.6073/pasta/c87ffaba606214a37ff3f932b3a0889b (Kohler 2018) and https://doi.org/10.6073/pasta/b217f5f36d18d149a8f52f17a7823f1d (Kohler and McKnight 2023).

Declarations

Competing interests The authors have no relevant financial or non-financial interests to disclose.

References

Alger AS, McKnight DM, Spaulding SA, Tate CM, Shupe GH, Welch KA, Edwards R, Andrews ED, House HR (1997) Ecological processes in a cold desert ecosystem: the abundance and species distribution of algal mats in glacial meltwater streams in Taylor Valley. Institute of Arctic and Alpine Research Occasional Paper: Antarctica. 51.

Bakker EA, Vizza C, Arango CP, Roley SS (2022) Nitrogen fixation rates in forested mountain streams: Are sediment microbes more important than previously thought? Freshw Biol 67:1395–1410. https://doi.org/10.1111/fwb.13925

Barr DM (1999) Biotic and abiotic regulation of nitrogen dynamics in biological soil crusts. Northern Arizona University.

Barrett JE, Virginia RA, Lyons WB, McKnight DM, Priscu JC, Doran PT, Fountain AG, Wall DH, Moorhead DL (2007) Biogeochemical stoichiometry of Antarctic Dry Valley ecosystems. J Geophys Res 112:G01010. https://doi.org/10.1029/2005JG000141

Bate DB, Barrett JE, Poage MA, Virginia RA (2008) Soil phosphorus cycling in an Antarctic polar desert. Geoderma 144:21–31. https://doi.org/10.1016/j.geoderma.2007.10.007

Bergstrom A, Gooseff M (2021) Chemical and sediment characteristics of ice cores collected from the ablation zones of Canada, Commonwealth, Howard, Hughes, and Seuss Glaciers in the McMurdo Dry Valleys, Antarctica from 2015 to 2019 ver 1. Environ Data Initiative. https://doi.org/10.6073/pasta/9943dc9f5b04e9d24424911c19349b58

Bergstrom AJ, Gooseff MN, Singley JG, Cohen MJ, Welch KA (2020) Nutrient Uptake in the Supraglacial Stream Network of an Antarctic Glacier. J Geophys Res Biogeosci. https://doi.org/10.1029/2020JG005679

Boulton AJ, Findlay S, Marmonier P, Stanley EH, Valett HM (1998) The functional significance of the hyporheic zone in streams and rivers. Annu Rev Ecol Syst 29(1):59–81. https://doi.org/10.1146/annurev.ecolsys.29.1.59

Burnham KP, Anderson DR (2002) Model Selection and Multimodel Inference: A Practical Information-Theoretic Approach. Springer, New York

Coyne KJ, Parker AE, Lee CK, Sohm JA, Kalmbach A, Gunderson T, León-Zayas R, Capone DG, Carpenter EJ, Cary SC (2020) The distribution and relative ecological roles of autotrophic and heterotrophic diazotrophs in the McMurdo Dry Valleys Antarctica. FEMS Microbiol Ecol. https://doi.org/10.1093/femsec/fiaa010

Cullis JDS, Stanish LF, McKnight DM (2014) Diel flow pulses drive particulate organic matter transport from microbial mats in a glacial meltwater stream in the McMurdo Dry Valleys. Water Resour Res 50:86–97. https://doi.org/10.1002/2013WR014061

Dodds WK, Gudder DA, Mollenhauer D (1995) The ecology of Nostoc. J Phycol 31:2–18. https://doi.org/10.1111/j.0022-3646.1995.00002.x

Dubnick A, Wadham JL, Tranter M, Sharp M, Orwin J, Barker J, Bagshaw E, Fitzsimons S (2017) Trickle or treat: the dynamics of nutrient export from polar glaciers. Hydrol Process 31:1776–1789. https://doi.org/10.1002/hyp.11149

Elser JJ, Wu C, González AL, Shain DH, Smith HJ, Sommaruga R, Williamson CE, Brahney J, Hotaling S, Vanderwall J, Yu J (2020) Key rules of life and the fading cryosphere: impacts in alpine lakes and streams. Glob Change Biol 26:6644–6656. https://doi.org/10.1111/gcb.15362

Findlay S (1995) Importance of surface-subsurface exchange in stream ecosystems: the hyporheic zone. Limnol Oceanogr 40(1):159–164. https://doi.org/10.4319/lo.1995.40.1.0159

Foreman CM, Wolf CF, Priscu JC (2004) Impact of episodic warming events on the physical, chemical, and biological relationships of lakes in the McMurdo Dry Valleys, Antarctica. Aquat Geochem 10:239–268. https://doi.org/10.1007/s10498-004-2261-3

Fountain AG, Lyons WB, Burkins MB, Dana GL, Doran PT, Lewis KJ, McKnight DM, Moorhead DL, Parsons AN, Priscu JC, Wall DH, Wharton RA, Virginia RA (1999) Physical controls on the Taylor Valley ecosystem, Antarctica. Bioscience 49:961–971. https://doi.org/10.1525/bisi.1999.49.12.961

Fowler D, Coyle M, Skiba U, Sutton MA, Cape JN, Reis S, Sheppard LJ, Jenkins A, Grizzetti B, Galloway JN,

Vitousek P (2013) The global nitrogen cycle in the twenty-first century. Philos Trans R Soc Lond B Biol Sci 368:20130164. https://doi.org/10.1098/rstb.2013.0164

Glibert PM, Bronk DA (1994) Release of dissolved organic nitrogen by marine diazotrophic cyanobacteria, Trichodesmium spp. App Environ Microbiol 60:3996–4000. https://doi.org/10.1128/aem.60.11.3996-4000.1994

Gooseff MN, McKnight DM, Lyons WB, Blum AE (2002) Weathering reactions and hyporheic exchange controls on stream water chemistry in a glacial meltwater stream in the McMurdo Dry Valleys. Water Resour Res 38:15–21. https://doi.org/10.1029/2001WR000834

Gooseff MN, McKnight DM, Runkel RL, Duff JH (2004) Denitrification and hydrologic transient storage in a glacial meltwater stream, McMurdo Dry Valleys, Antarctica. Limnol Oceanogr 49:1884–1895. https://doi.org/10.4319/lo.2004.49.5.1884

Gooseff MN, Barrett JE, Adams BJ, Doran PT, Fountain AG, Lyons WB, McKnight DM, Priscu JC, Sokol ER, Takacs-Vesbach C, Vandegehuchte ML, Virginia RA, Wall DH (2017) Decadal ecosystem response to an anomalous melt season in a polar desert in Antarctica. Nat Ecol Evol 1:1334–1338. https://doi.org/10.1038/s41559-017-0253-0

Grimm NB, Petrone KC (1997) Nitrogen fixation in a desert stream ecosystem. Biogeochemistry 37:33–61. https://doi.org/10.1023/A:1005798410819

Harris D, Horwáth WR, van Kessel C (2001) Acid fumigation of soils to remove carbonates prior to total organic carbon or carbon-13 isotopic analysis. Soil Sci Soc Am J 65:1853–1856. https://doi.org/10.2136/sssaj2001.1853

Hedges JI, Stern JH (1984) Carbon and nitrogen determinations of carbonate containing solids. Limnol Oceanogr 29:657–663. https://doi.org/10.4319/lo.1984.29.3.0657

Heindel RC, Lyons WB, Welch SA, Spickard AM, Virginia RA (2018) Biogeochemical weathering of soil apatite grains in the McMurdo Dry Valleys, Antarctica. Geoderma 320:136–145. https://doi.org/10.1016/j.geoderma.2018.01.027

Heindel RC, Darling JP, Singley JG, Bergstrom AJ, McKnight DM, Lukkari BM, Welch KA, Gooseff MN (2021) Diatoms in hyporheic sediments trace organic matter retention and processing in the McMurdo Dry Valleys Antarctica. J Geophys Res Biogeosci. https://doi.org/10.1029/2020JG006097

Howard-Williams C, Priscu JC, Vincent WF (1989) Nitrogen dynamics in two Antarctic streams. Hydrobiologia 172:51–61. https://doi.org/10.1007/BF00031612

Johnson LT, Tank JL, Hall Jr RO, Mulholland PJ, Hamilton SK, Valett HM, Webster JR, Bernot MJ, McDowell WH, Peterson BJ, Thomas SM (2013) Quantifying the production of dissolved organic nitrogen in headwater streams using 15N tracer additions. Limnol Oceanogr 58(4):1271–1285. https://doi.org/10.4319/lo.2013.58.4.1271

Jones JB Jr, Fisher SG, Grimm NB (1995a) Nitrification in the hyporheic zone of a desert stream ecosystem. J North Am Benthol Soc 14:249–258. https://doi.org/10.2307/1467777

Jones JB Jr, Fisher SG, Grimm NB (1995b) Vertical hydrologic exchange and ecosystem metabolism in a Sonoran Desert stream. Ecology 76:942–952. https://doi.org/10.2307/1939358

Koch JC, McKnight DM, Baeseman JL (2010) Effect of unsteady flow on nitrate loss in an oligotrophic, glacial meltwater stream. J Geophys Res Biogeosci 115:G01001. https://doi.org/10.1029/2009JG001030

Kohler T (2018) McMurdo Dry Valleys Microbial mat biomass, isotopes, and nutrient ratios sampled over a longitudinal gradient of two McMurdo Dry Valley streams ver 2. Environ Data Initiative. https://doi.org/10.6073/pasta/c87ffaba606214a37ff3f932b3a0889b

Kohler TJ, McKnight DM (2023) Biomass, stoichiometry, and isotopic signatures of stream microbial mats, McMurdo Dry Valleys, Antarctica (2012–2013). Environ Data Initiative. https://doi.org/10.6073/pasta/b217f5f36d18d149a8f52f17a7823f1d

Kohler TJ, Chatfield E, Gooseff MN, Barrett JE, McKnight DM (2015a) Recovery of Antarctic stream epilithon from simulated scouring events. Antarct Sci 27:341–354. https://doi.org/10.1017/S0954102015000024

Kohler TJ, Stanish LF, Crisp SW, Koch JC, Liptzin D, Baseman JL, McKnight DM (2015b) Life in the main channel: long-term hydrologic control of microbial mat abundance in McMurdo Dry Valley streams, Antarctica. Ecosystems 18:310–327. https://doi.org/10.1007/s10021-014-9829-6

Kohler TJ, Van Horn DJ, Darling JP, Takacs-Vesbach CD, McKnight DM (2016) Nutrient treatments alter microbial mat colonization in two glacial meltwater streams from the McMurdo Dry Valleys Antarctica. FEMS Microbiol Ecol. https://doi.org/10.1093/femsec/fiw049

Kohler TJ, Stanish LF, Liptzin D, Barrett JE, McKnight DM (2018) Catch and release: hyporheic retention and mineralization of N-fixing *Nostoc* sustains downstream microbial mat biomass in two polar desert streams. Limnol Oceanogr Lett. https://doi.org/10.1002/lol2.10087

Kunza LA, Hall RO (2014) Nitrogen fixation can exceed inorganic nitrogen uptake fluxes in oligotrophic streams. Biogeochemistry 121:537–549. https://doi.org/10.1007/s10533-014-0021-z

Lehmann MF, Reichert P, Bernasconi SM, Barbieri A, McKenzie JA (2003) Modelling nitrogen and oxygen isotope fractionation during denitrification in a lacustrine redox-transition zone. Geochim Cosmochim Acta 67:2529–2542. https://doi.org/10.1016/S0016-7037(03)00085-1

Leslie DL, Welch K, Lyons WB (2017) A temporal stable isotopic (δ18O, δD, d-excess) comparison in glacier meltwater streams (Von Guerard Stream and Andersen Creek), Taylor Valley, Antarctica. Hydrol Process 31:3069–3083. https://doi.org/10.1002/hyp.11245

Marcarelli AM, Baker MA, Wurtsbaugh WA (2008) Is in-stream N2 fixation an important N source for benthic communities and stream ecosystems? J North Am Benthol Soc 27:186–211. https://doi.org/10.1899/07-027.1

Marcarelli AM, Fulweiler RW, Scott JT (2022) Nitrogen fixation: a poorly understood process along the freshwater-marine continuum. Limnol Oceanogr Lett 7:1–10. https://doi.org/10.1002/lol2.10220

Maurice PA, McKnight DM, Gooseff MN, Leff L, Fulghum JE (2002) Direct observations of aluminosilicate weathering in the hyporheic zone of an Antarctic dry valley stream. Geochim Cosmochim Acta 66:1335–1347

Mayland HF, McIntosh TH, Fuller WH (1966) Fixation of Isotopic Nitrogen on a Semiarid Soil by Algal Crust

Organisms. Soil Sci Soc Am J 30(15):956–960. https://doi.org/10.2136/sssaj1966.03615995003000010022x
McKnight DM, Niyogi DK, Alger AS, Bomblies A, Conovitz PA, Tate CM (1999) Dry valley streams in Antarctica: ecosystems waiting for water. Bioscience 49:985–995. https://doi.org/10.1525/bisi.1999.49.12.985
McKnight DM, Runkel RL, Tate CM, Duff JH, Moorhead DL (2004) Inorganic N and P dynamics of Antarctic glacial meltwater streams as controlled by hyporheic exchange and benthic autotrophic communities. J North Am Benthol Soc 23:171–188. https://doi.org/10.1899/0887-3593(2004)023%3c0171:INAPDO%3e2.0.CO;2
McKnight DM, Tate CM, Andrews ED, Niyogi DK, Cozzetto K, Welch K, Lyons WB, Capone DG (2007) Reactivation of a cryptobiotic stream ecosystem in the McMurdo Dry Valleys, Antarctica: A long-term geomorphological experiment. Geomorphology 89:186–204. https://doi.org/10.1016/j.geomorph.2006.07.025
Michalski G, Bockheim JG, Kendall C, Thiemens M (2005) Isotopic composition of Antarctic Dry Valley nitrate: Implications for NOy sources and cycling in Antarctica. Geophys Res Lett 32:L13817. https://doi.org/10.1029/2004GL022121
Michener R, Lajtha K (2007) Stable isotopes in ecology and environmental science, 2nd edn. Blackwell, Oxford, p 566
Krause S, Hannah DM, Fleckenstein JH, Heppell CM, Kaeser D, Pickup R, Pinay G, Robertson AL, Wood PJ (2011) Inter-disciplinary perspectives on processes in the hyporheic zone. Ecohydrology 4(4):481–499. https://doi.org/10.1002/eco.176
Montoya JP, McCarthy JJ (1995) Isotopic fractionation during nitrate uptake by phytoplankton grown in continuous culture. J Plank Res 17(3):439–464. https://doi.org/10.1093/plankt/17.3.439
Murphy J, Riley JP (1962) A modified single solution method for determination of phosphate in natural waters. Anal Chim Acta 26:31–36. https://doi.org/10.1016/S0003-2670(00)88444-5
Myrstener M, Rocher-Ros G, Burrows RM, Bergström AK, Giesler R, Sponseller RA (2018) Persistent nitrogen limitation of stream biofilm communities along climate gradients in the Arctic. Glob Change Biol 24:3680–3691. https://doi.org/10.1111/gcb.14117
Newbold D, Elwood JW, O'Neill RV, Van Winkle W (1981) Measuring nutrient spiraling in streams. Can J Fish Aquat Sci 38:860–863. https://doi.org/10.1139/f81-114
O'Brien JM, Hamilton SK, Podzikowski L, Ostrom N (2012) The fate of assimilated nitrogen in streams: an in situ benthic chamber study. Freshwater Biol 57(6): 1113–1125. https://doi.org/10.1111/j.1365-2427.2012.02770.x
Peterson BJ, Fry B (1987) Stable isotopes in ecosystem studies. Annu Rev Ecol Syst 18:293–320
Peterson BJ, Bahr M, Kling GW (1997) A tracer investigation of nitrogen cycling in a pristine tundra river. Can J Fish Aquat Sci 54:2361–2367. https://doi.org/10.1139/f97-142
Priscu JC (1995) Phytoplankton nutrient deficiency in lakes of the McMurdo Dry Valleys, Antarctica. Freshw Biol 34:215–227. https://doi.org/10.1111/j.1365-2427.1995.tb00882.x
R Core Team. 2022. R: A language and environment for statistical computing. R Foundation for Statistical Computing. Available from http://www.R-project.org/.
Redfield A (1958) The biological control of chemical factors in the environment. Am Sci 46:205–221
Ren Z, Martyniuk N, Oleksy IA, Swain A, Hotaling S (2019) Ecological stoichiometry of the mountain cryosphere. Front Ecol Evol 7:360. https://doi.org/10.3389/fevo.2019.00360
Runkel RL, McKnight DM, Andrews ED (1998) Analysis of transient storage subject to unsteady flow: diel flow variation in an Antarctic stream. J North Am Benthol Soc 17:143–154
Scott JT, Doyle RD, Back JA, Dworkin SI (2007) The role of N_2 fixation in alleviating N limitation in wetland metaphyton: enzymatic, isotopic, and elemental evidence. Biogeochemistry 84:207–218. https://doi.org/10.1007/s10533-007-9119-x
Singley JG, Gooseff MN, McKnight DM, Hinckley ES (2021) The role of hyporheic connectivity in determining nitrogen availability: insights from an intermittent Antarctic stream. J Geophys Res Biogeosci. https://doi.org/10.1029/2021JG006309
Singley JG, Salvatore MR, Gooseff MN, McKnight DM, Hinckley ELS (2023) Differentiating physical and biological storage of N along an intermittent Antarctic stream corridor. Freshw Sci. https://doi.org/10.1086/725676
Sohm J, Niederberger T, Parker A, Tirindelli J, Gunderson T, Cary S, Capone D, Carpenter E (2020) Microbial mats of the McMurdo Dry Valleys, Antarctica: oases of biological activity in a very cold desert. Front Microbiol. https://doi.org/10.3389/fmicb.2020.537960
Stanish LF. Ecological controls on stream diatom communities in the McMurdo Dry Valleys, Antarctica. *PhD Dissertation*. University of Colorado 2011.
Steinman A, Lamberti GA, Leavitt PR (1996) Biomass and pigments of benthic algae. In: Hauer FR, Lamberti GA (eds) Methods in stream ecology, 2nd edn. Academic Press, San Diego, pp 357–379
Valett HM, Fisher SG, Grimm NB, Camill P (1994) Vertical hydrologic exchange and ecological stability of a desert stream ecosystem. Ecology 75:548–560. https://doi.org/10.2307/1939557
Van Horn DJ, Wolf CR, Colman DR, Jiang X, Kohler TJ, McKnight DM, Stanish LF, Yazzie T, Takacs-Vesbach CD (2016) Patterns of bacterial biodiversity in the glacial meltwater streams of the McMurdo Dry Valleys Antarctica. FEMS Microbiol Ecol. https://doi.org/10.1093/femsec/fiw148
Vitousek PM, Aber JD, Howarth RW, Likens GE, Matson PA, Schindler DW, Schlesinger WH, Tilman DG (1997) Human alteration of the global nitrogen cycle: Sources and consequences. Bioscience 7:737–750. https://doi.org/10.1890/1051-0761(1997)007[0737:HAOTGN]2.0.CO;2
Welch KA, Lyons WB, Whisner C, Gardner CB, Gooseff MN, McKnight DM, Priscu JC (2010) Spatial variations in the geochemistry of glacial meltwater streams in the Taylor Valley, Antarctica. Antarct Sci 22:662–672. https://doi.org/10.1017/S0954102010000702

Welschmeyer NA (1994) Fluorometric analysis of chlorophyll a in the presence of chlorophyll b and pheopigments. Limnol Oceanogr 39:1985–1992. https://doi.org/10.4319/lo.1994.39.8.1985

Welter JR, Benstead JP, Cross WF, Hood JM, Huryn AD, Johnson PW, Williamson TJ (2015) Does N2 fixation amplify the temperature dependence of ecosystem metabolism? Ecology 96:603–610. https://doi.org/10.1890/14-1667.1

Wlostowski AN, Gooseff MN, McKnight DM, Jaros C, Lyons WB (2016) Patterns of hydrologic connectivity in the McMurdo Dry Valleys, Antarctica: a synthesis of 20 years of hydrologic data. Hydrol Process. https://doi.org/10.1002/hyp.10818.10.1002/hyp.10818

Zoumplis A, Kolody B, Kaul D, Zheng H, Venepally P, McKnight DM, Takacs-Vesbach C, DeVries A, Allen AE (2023) Impact of meltwater flow intensity on the spatiotemporal heterogeneity of microbial mats in the McMurdo Dry Valleys Antarctica. ISME Comm. https://doi.org/10.1038/s43705-022-00202-8

Zuur AF, Ieno EN, Walker NJ, Saveliev AA, Smith GM (2009) Mixed effects models and extensions in ecology with R. Springer, New York, p 574

Zuur AF, Ieno EN, Elphick CS (2010) A protocol for data exploration to avoid common statistical problems. Methods Ecol Evol 1:3–14. https://doi.org/10.1111/j.2041-210X.2009.00001.x